Supporting Information

Rational synthesis of luminescent uncommon (3,4,6)-c connected Zn(II) MOF: a dual channel sensor for the detection of nitroaromatics and ferric ion

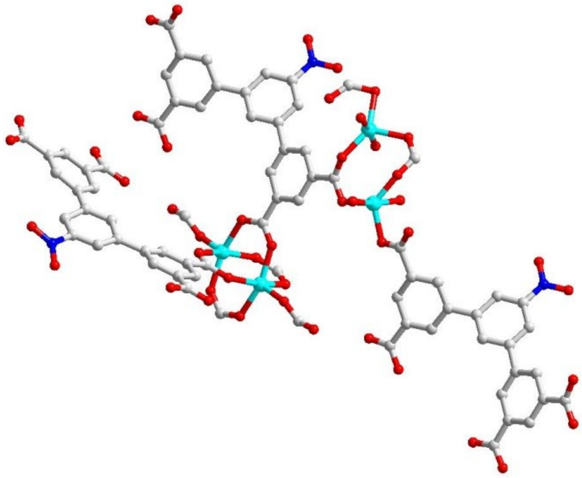

Fig. S1 view of the two types of binuclear [$Zn_2(\mu_2\text{-}COO)_2(\mu_1\text{-}COO)_2$] and [$Zn_2(\mu_2\text{-}COO)_4$].

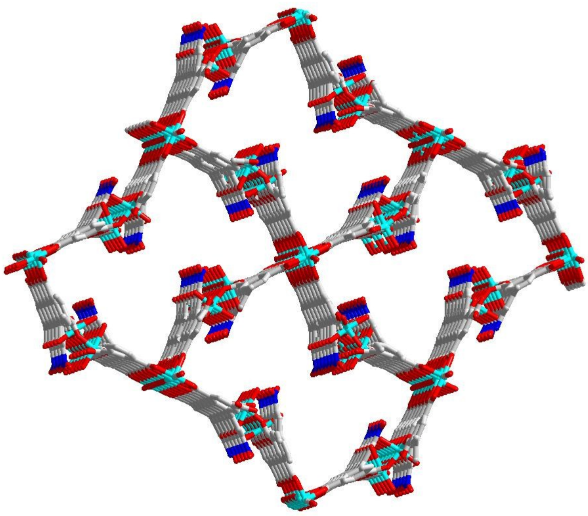

Fig. S2 The 3D porous structure of 1 along the *a* axis.

Thermogravimetric analysis (TGA) for **1** shows a weight loss of 22.6 % between 35 and 285 °C, which corresponding to the loss of 5.5 DMF and coordinated H_2O molecules. Upon further heating, a weight loss of 34.9 % should correspond to the release of the organic ddn and formate ligands, and then the collapse of the framework (calcd 32.8 %) (Fig.S3). Anal. (%) calcd for $C_{62.4}H_{75.6}N_{8.8}O_{31.6}Zn_4$: C, 43.56 %; H, 4.43 %; N, 7.17 %; Found: C, 42.66 %; H, 4.01%; N, 6.87 %.

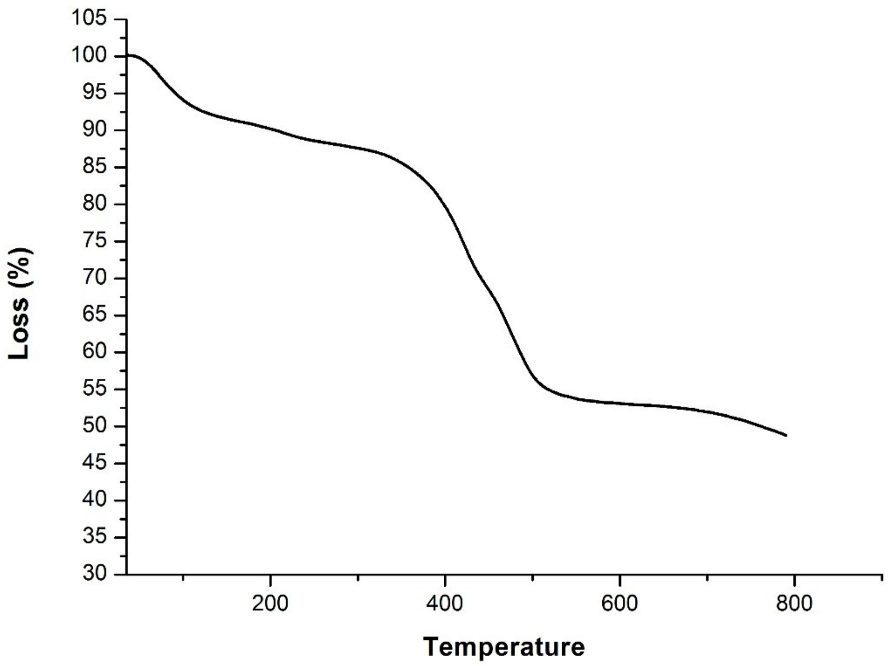

Fig. S3 view of the TGA.

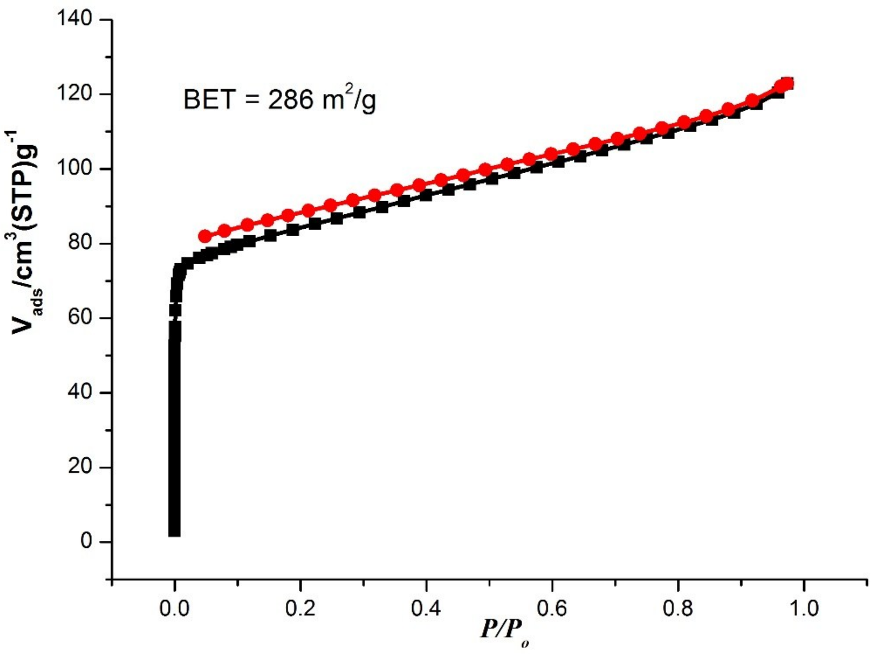

Fig. S4 view of the N_2 adsorption isotherms at 77 K.

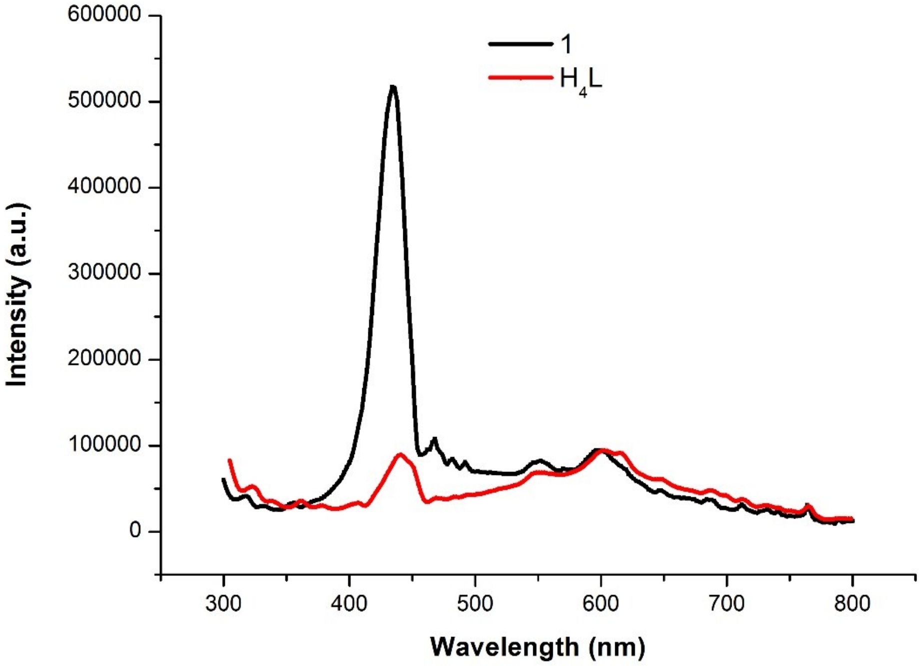

Fig. S5 The photoluminescence spectra of solid samples of H_4ddn ligand and **1** recorded at room temperature.

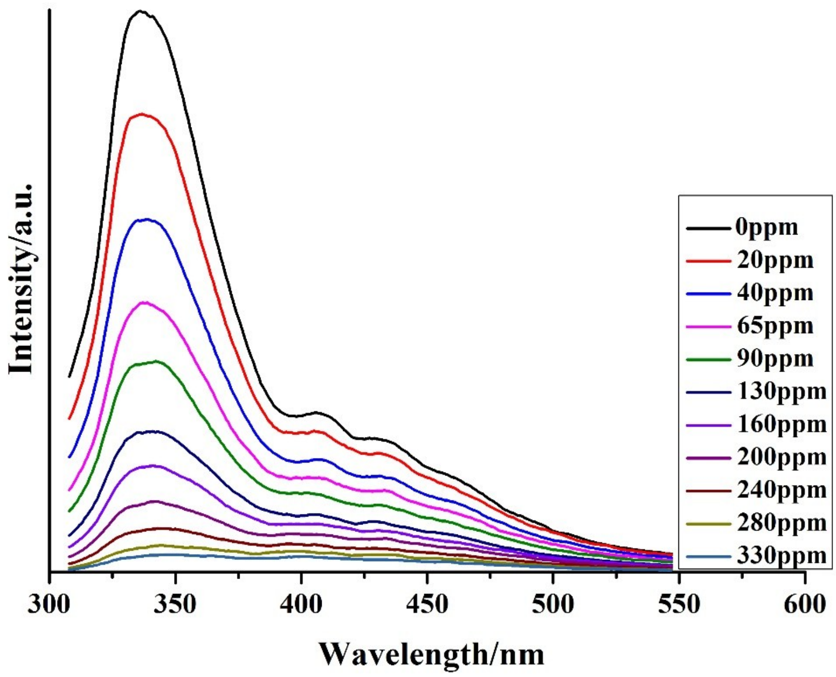

Fig. S6 Luminescent quenching of **1** dispersed in ethanol by the gradual addition of 1 mM solution of 1,3-DNB in DMF.

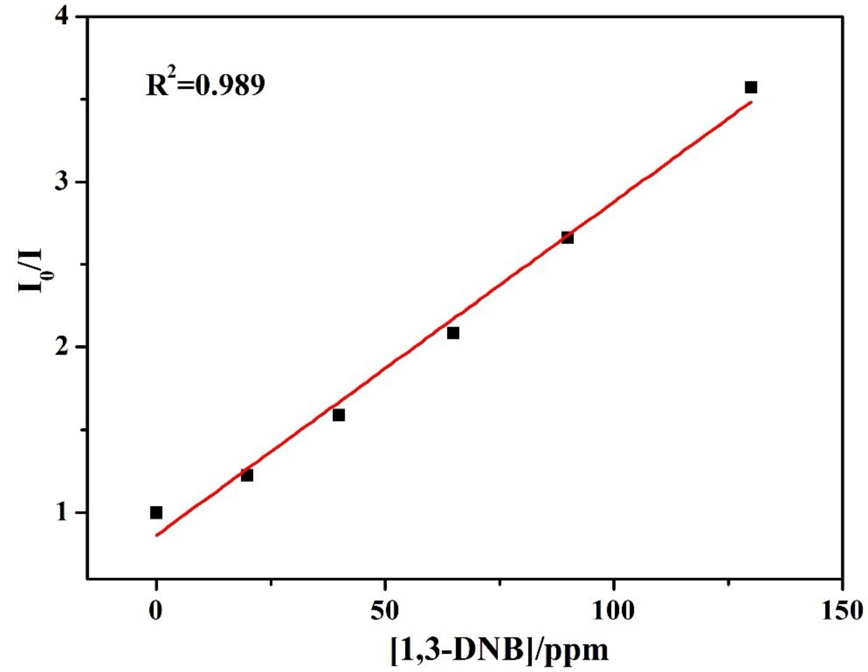

Fig. S7 The Stern–Volmer plot of **1** against 1,3-DNB.

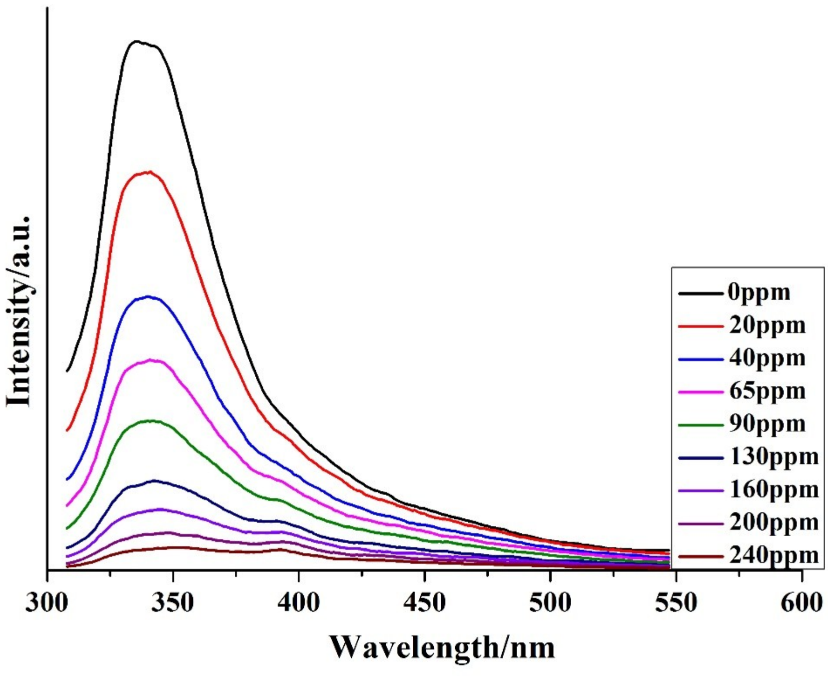

Fig. S8 Luminescent quenching of **1** dispersed in ethanol by the gradual addition of 1 mM solution of 2,4-DNT in DMF.

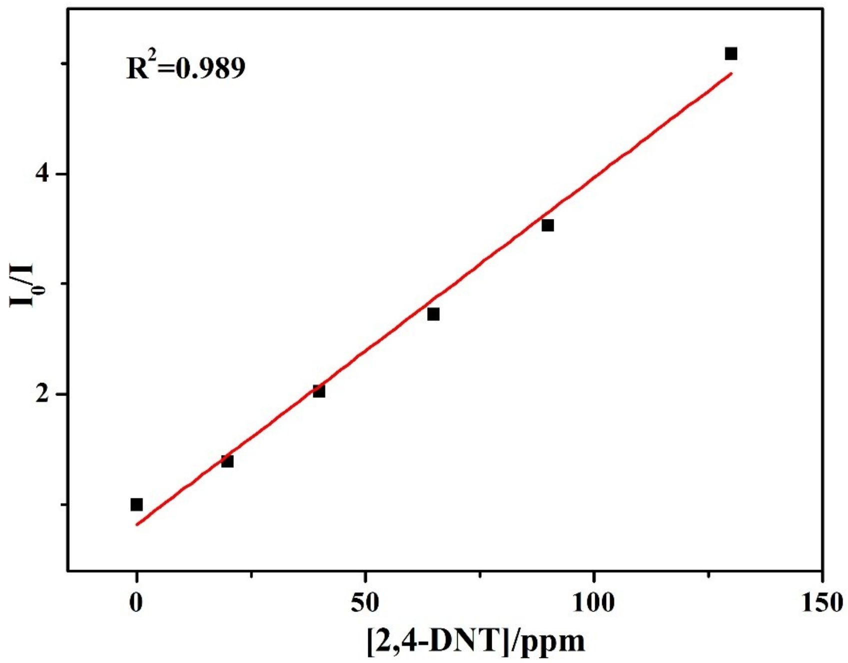

Fig. S9 Stern–Volmer plot for the fluorescence quenching of **1** upon the addition of 2,4-DNT.

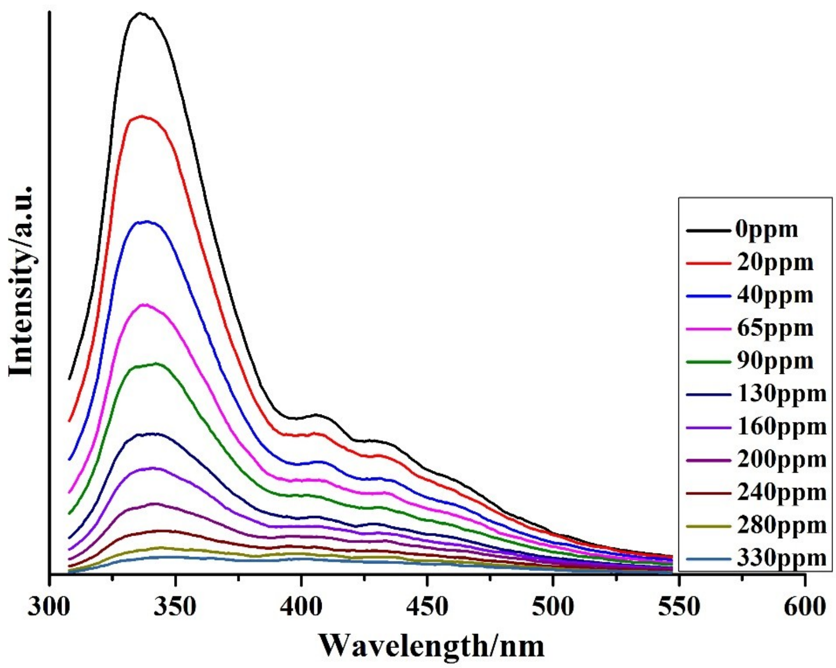

Fig. S10 Luminescent quenching of **1** dispersed in ethanol by the gradual addition of 1 mM solution of 2,6-DNT in DMF.

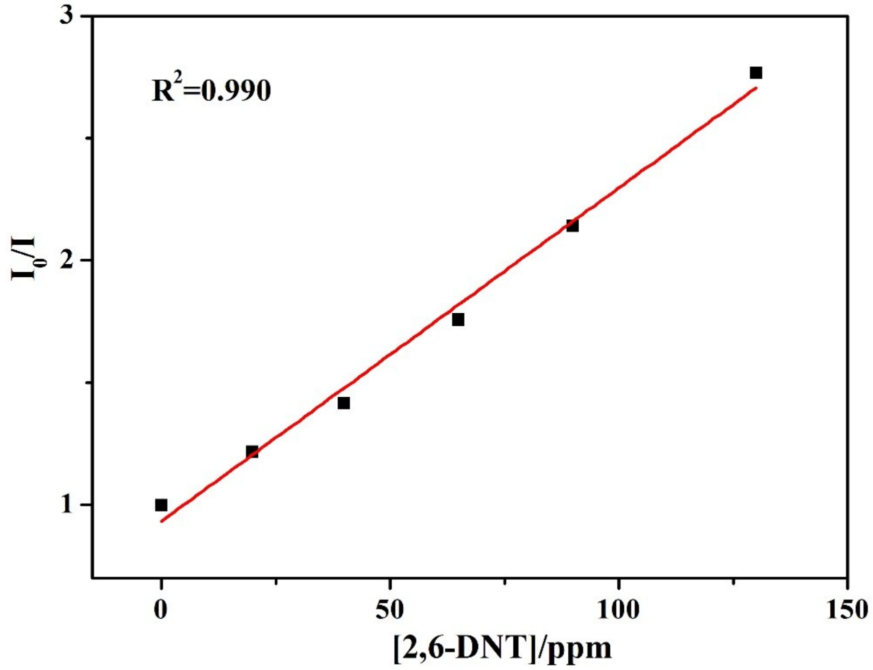

Fig. S11 Stern–Volmer plot for the fluorescence quenching of **1** upon the addition of 2,6-DNT.

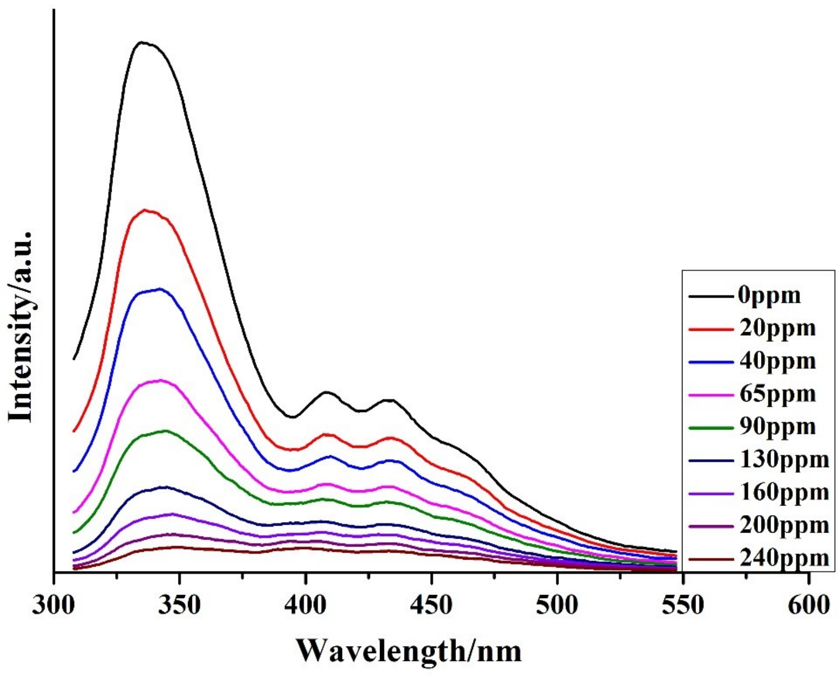

Fig. S12 Luminescent quenching of **1** dispersed in ethanol by the gradual addition of 1 mM solution of 2-NT in DMF.

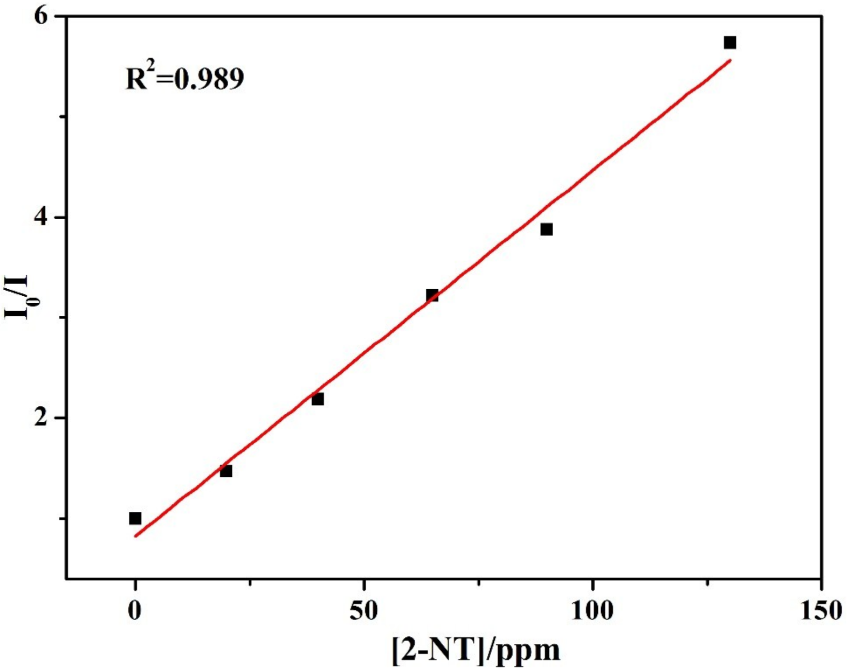

Fig. S13 Stern–Volmer plot for the fluorescence quenching of **1** upon the addition of 2-NT.

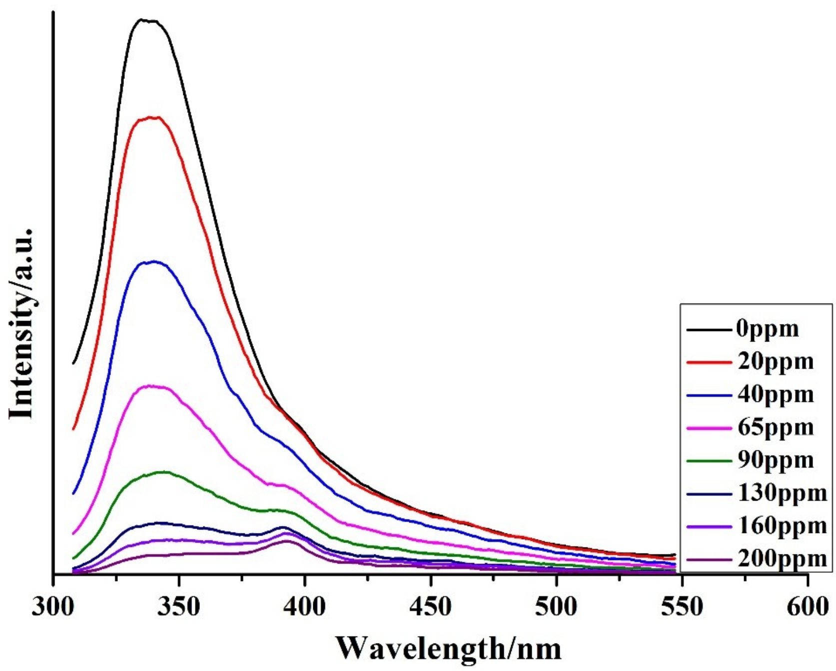

Fig. S14 Luminescent quenching of **1** dispersed in ethanol by the gradual addition of 1 mM solution of 4-NT in DMF.

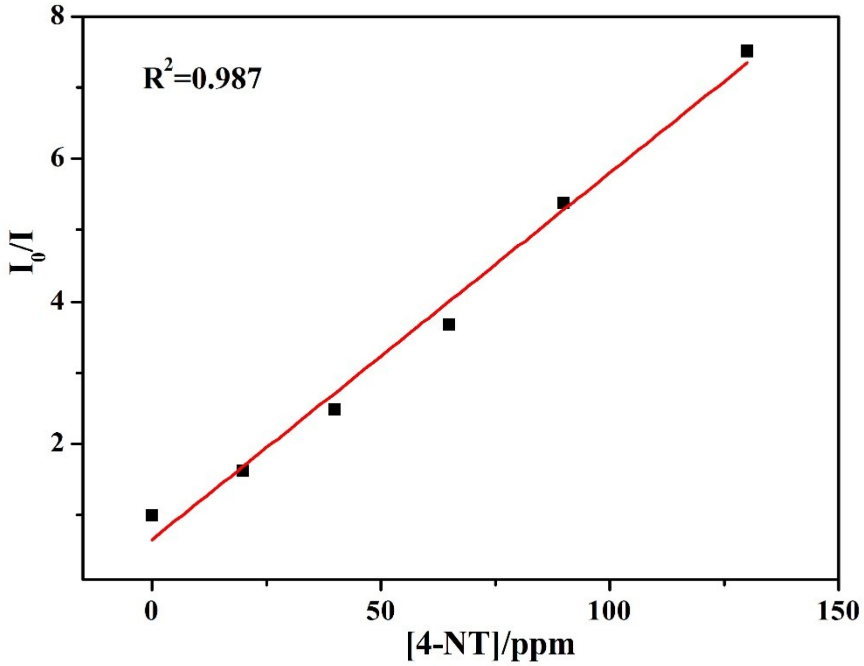

Fig. S15 Stern–Volmer plot for the fluorescence quenching of **1** upon the addition of 4-NT.

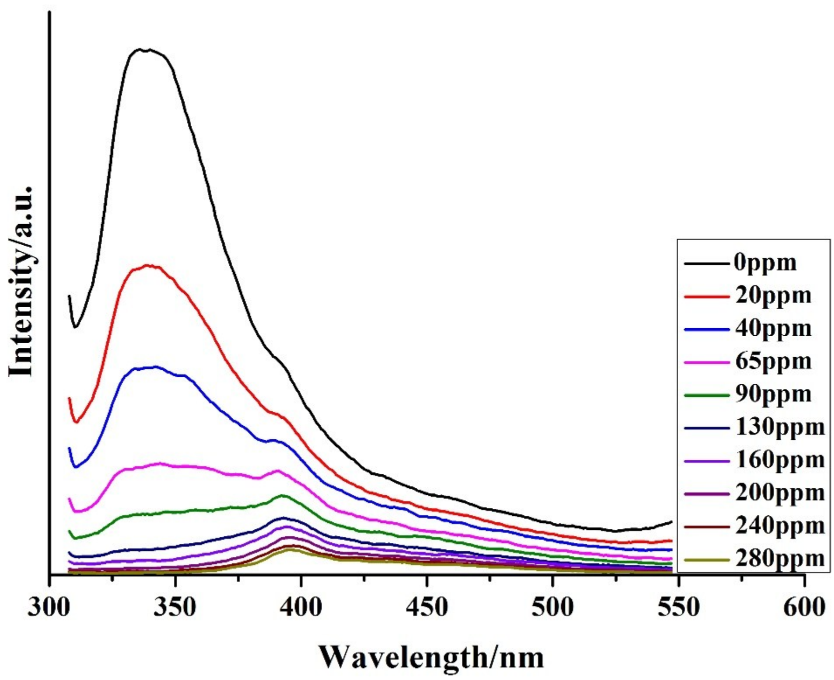

Fig. S16 Stern–Volmer plot for the fluorescence quenching of **1** upon the addition of MNP.

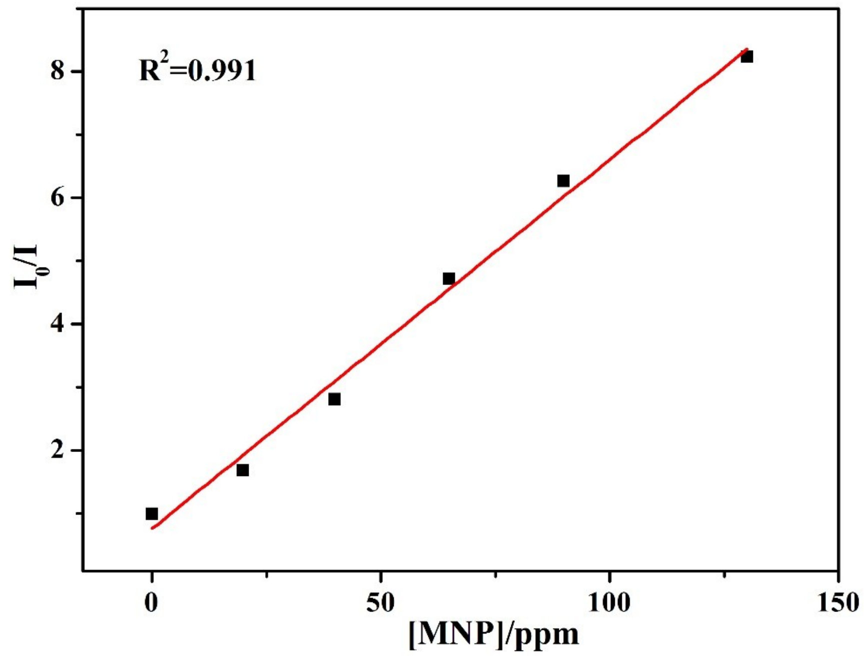

Fig. S17 Stern–Volmer plot for the fluorescence quenching of **1** upon the addition of MNP.

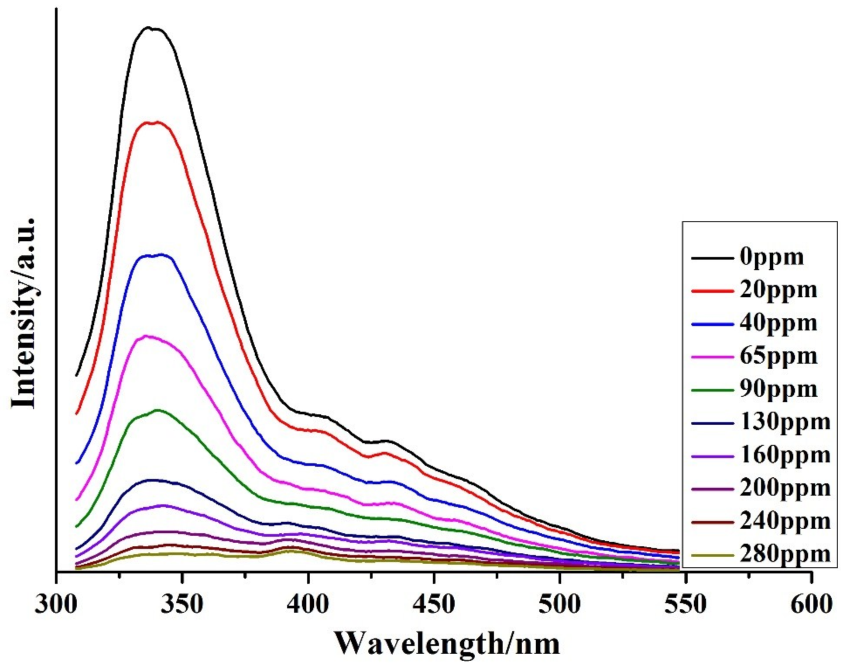

Fig. S18 Luminescent quenching of **1** dispersed in ethanol by the gradual addition of 1 mM solution of NB in DMF.

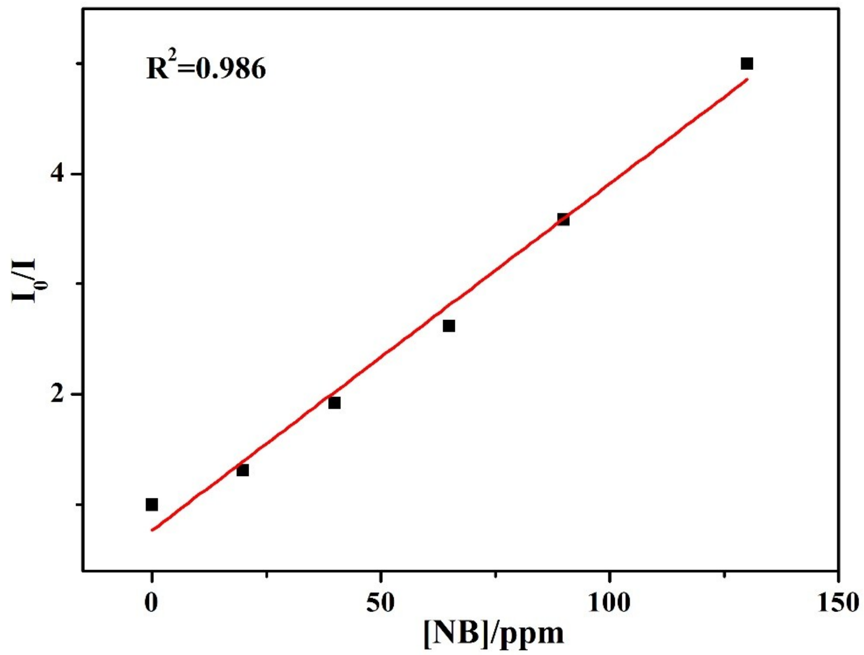

Fig. S19 Stern–Volmer plot for the fluorescence quenching of **1** upon the addition of NB.

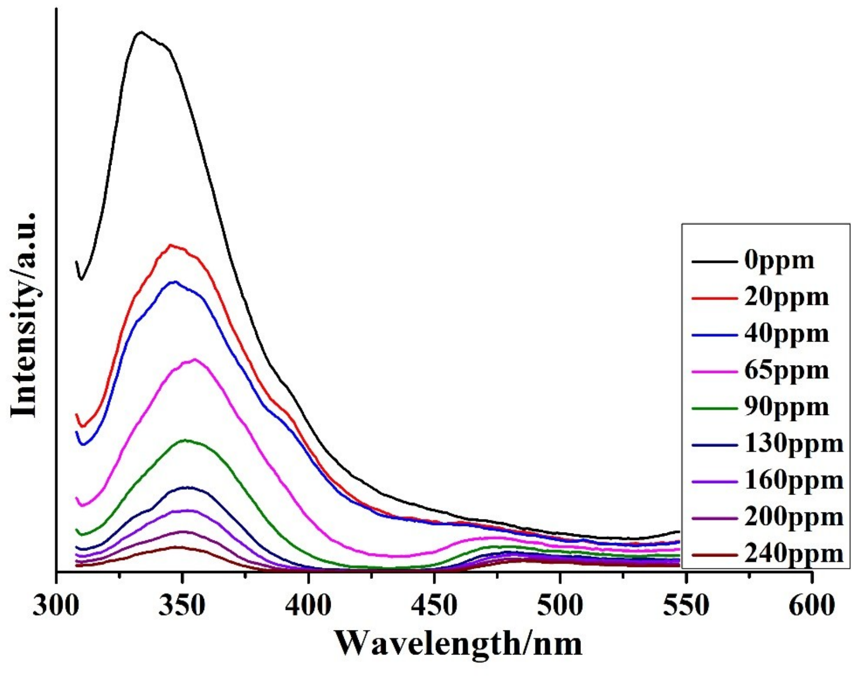

Fig. S20 Luminescent quenching of **1** dispersed in ethanol by the gradual addition of 1 mM solution of PNP in DMF.

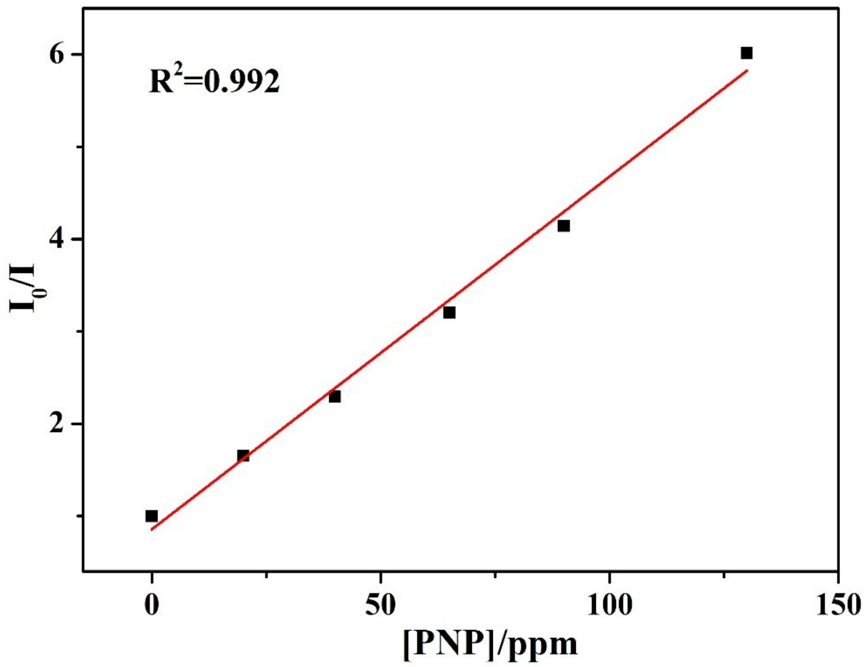

Fig. S21 Stern–Volmer plot for the fluorescence quenching of **1** upon the addition of PNP.

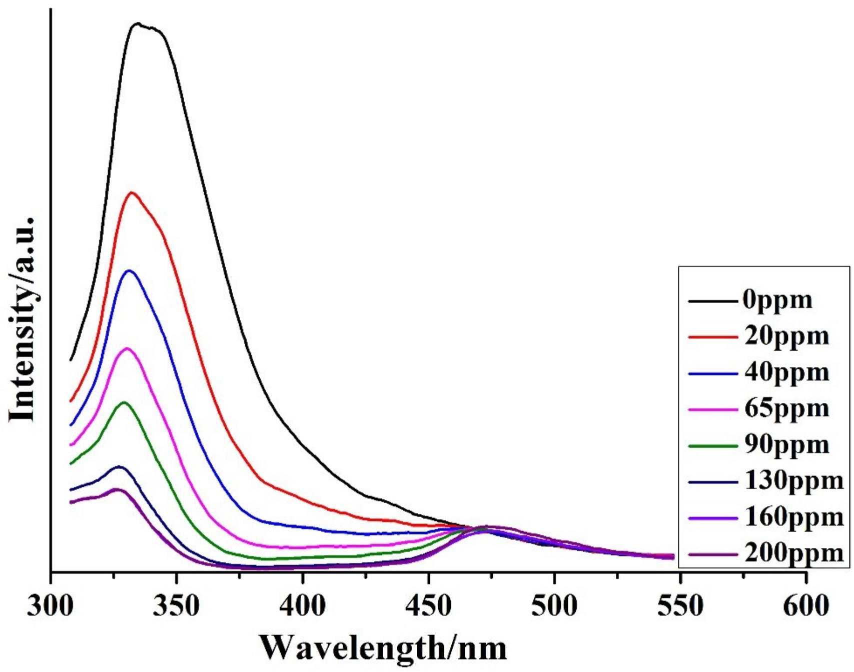

Fig. S22 Luminescent quenching of **1** dispersed in ethanol by the gradual addition of 1 mM solution of TNP in DMF.

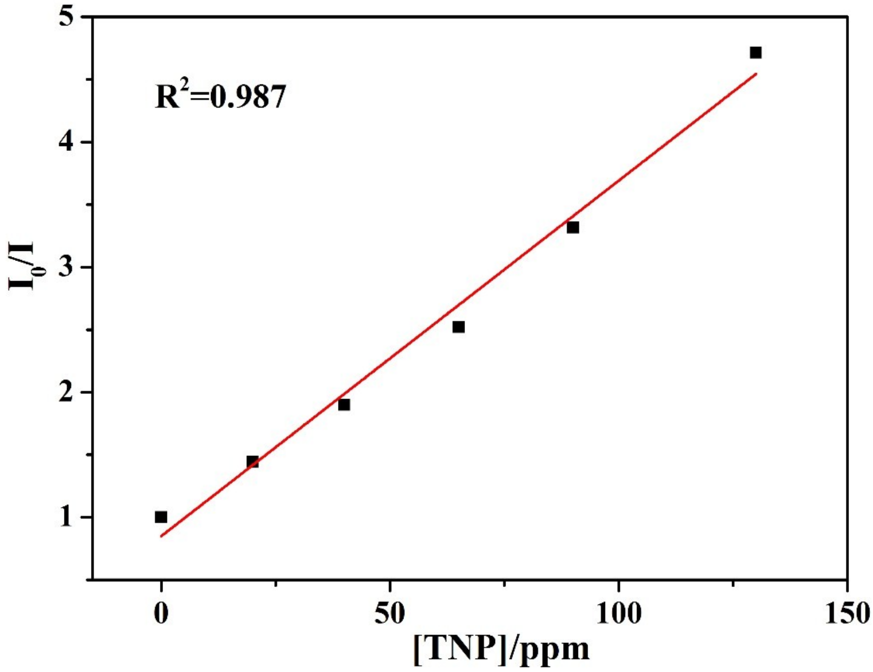

Fig. S23 Stern–Volmer plot for the fluorescence quenching of **1** upon the addition of TNP.

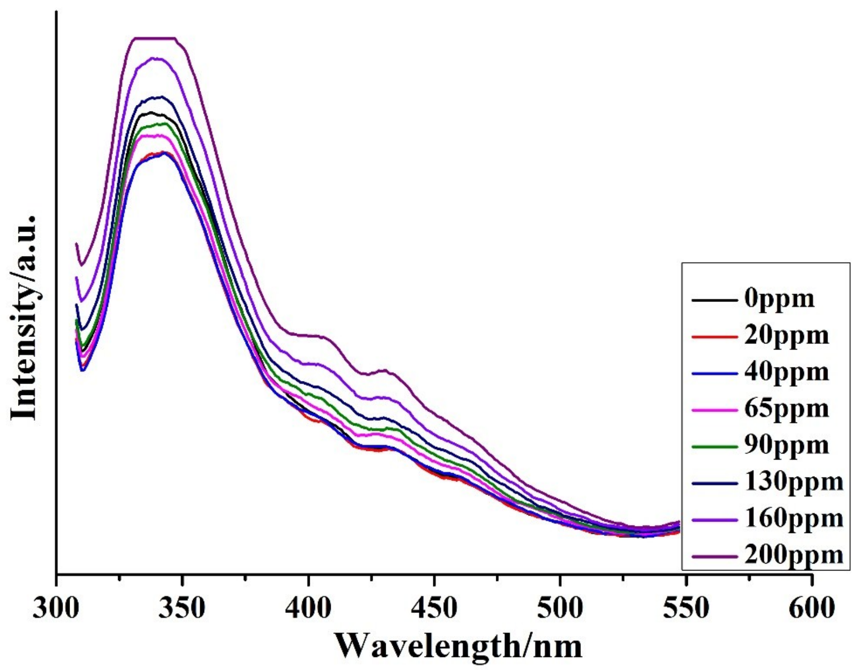

Fig. S24 Luminescent quenching of **1** dispersed in ethanol by the gradual addition of 1 mM solution of 1,2,4-TMB in DMF.

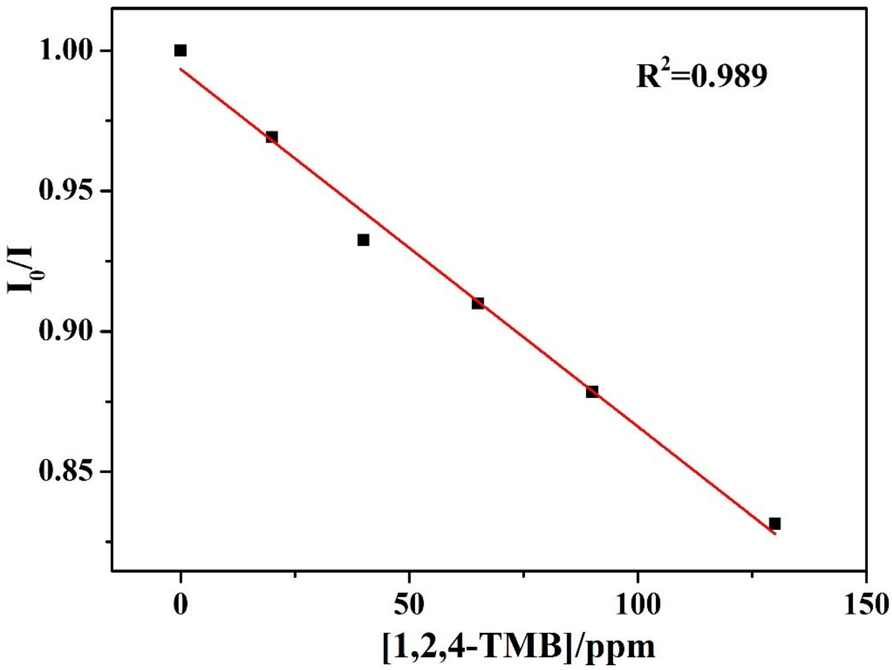

Fig. S25 Stern–Volmer plot for the fluorescence quenching of **1** upon the addition of 1,2,4-TMB.

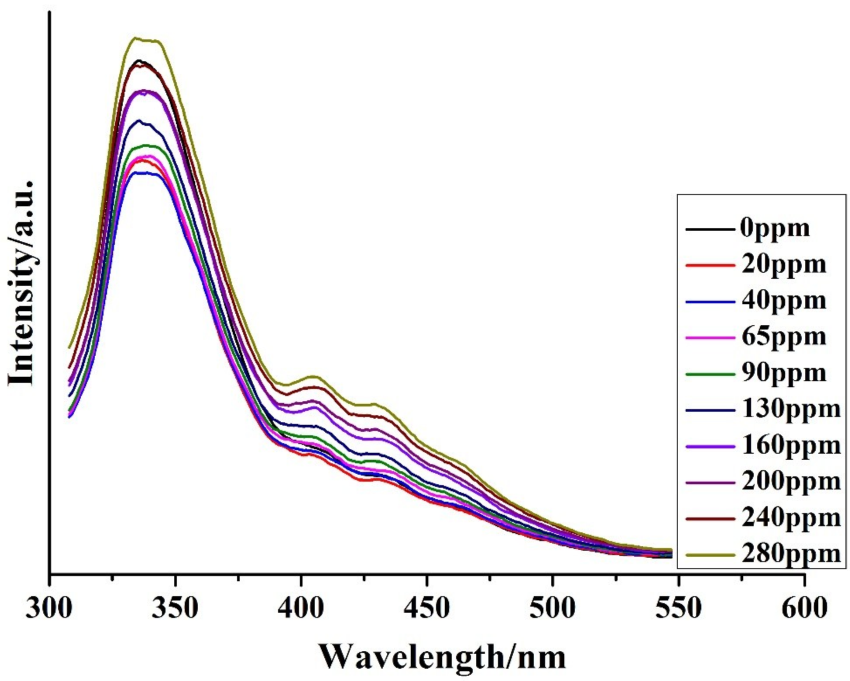

Fig. S26 Luminescent quenching of **1** dispersed in ethanol by the gradual addition of 1 mM solution of 1,3,5-TMB in DMF.

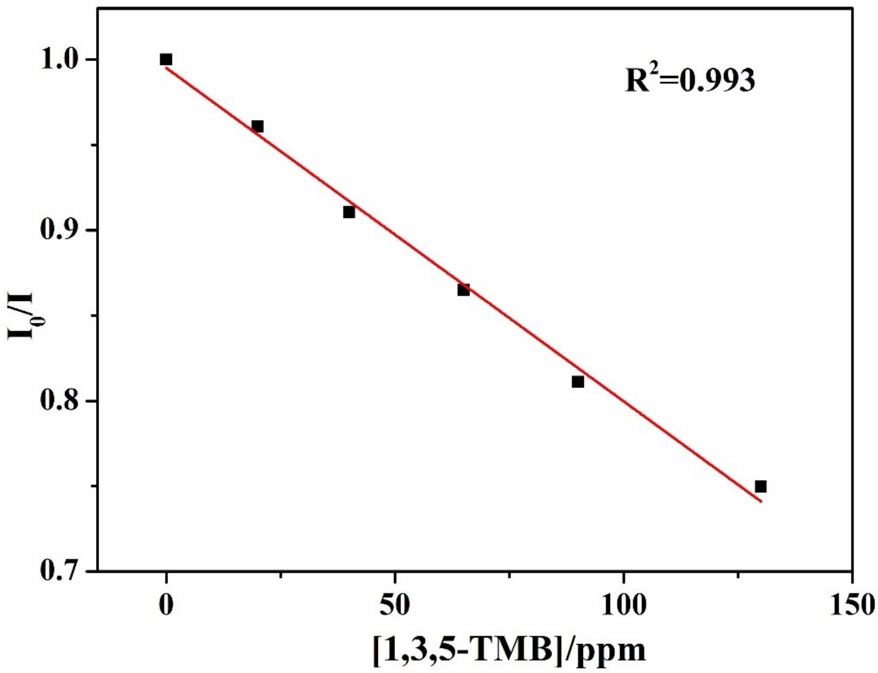

Fig. S27 Stern–Volmer plot for the fluorescence quenching of **1** upon the addition of 1,3,5-TMB.

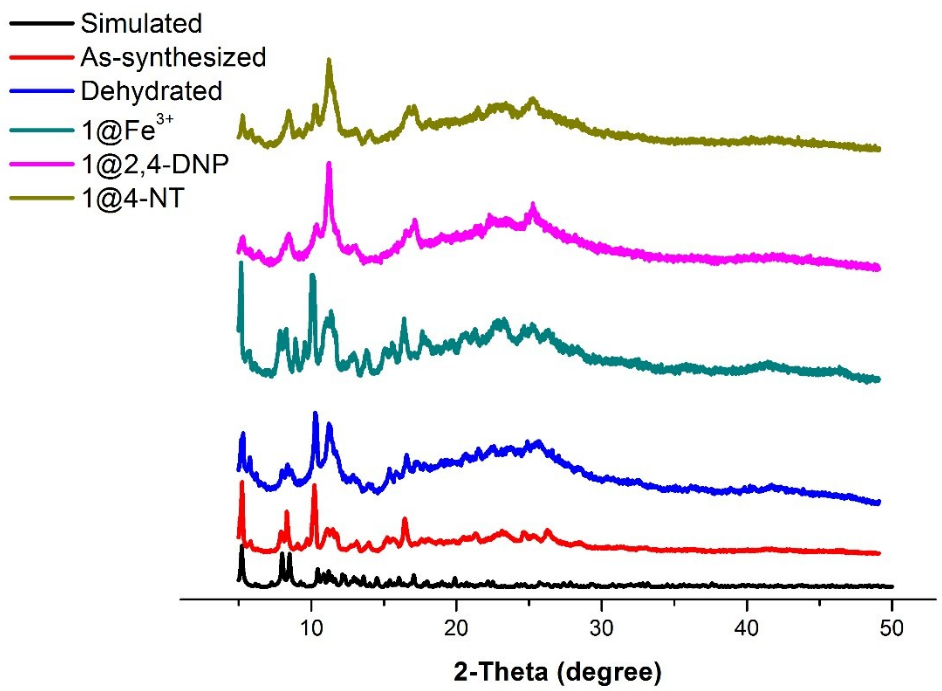

Fig. S28 view of the PXRD for the sample **1** (black: simulated; red: as-synthesized) and its suspensions of analytes.

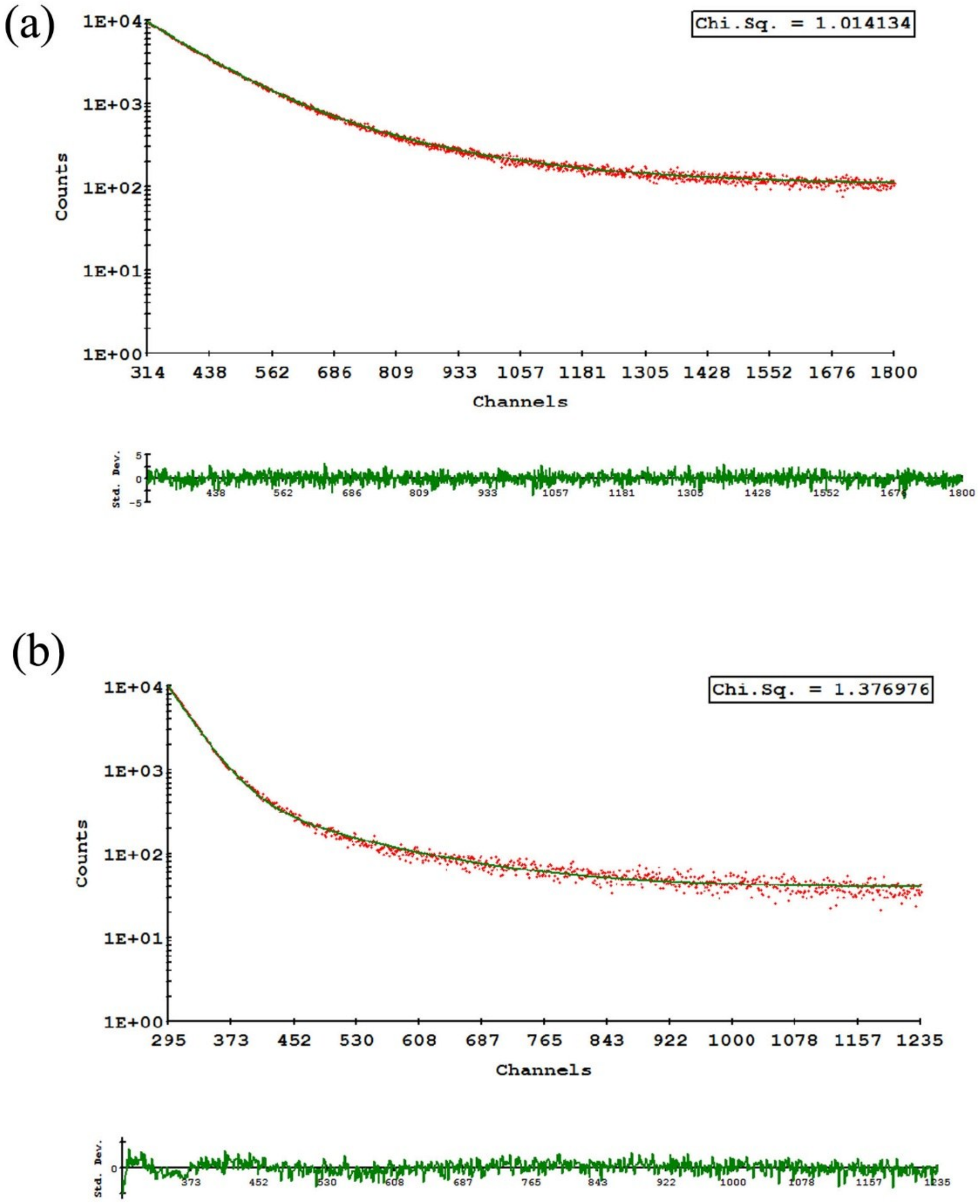

Fig. S29 Comparison of the fluorescence lifetime of **1** (above) and Fe^{3+}@ **1** (below).

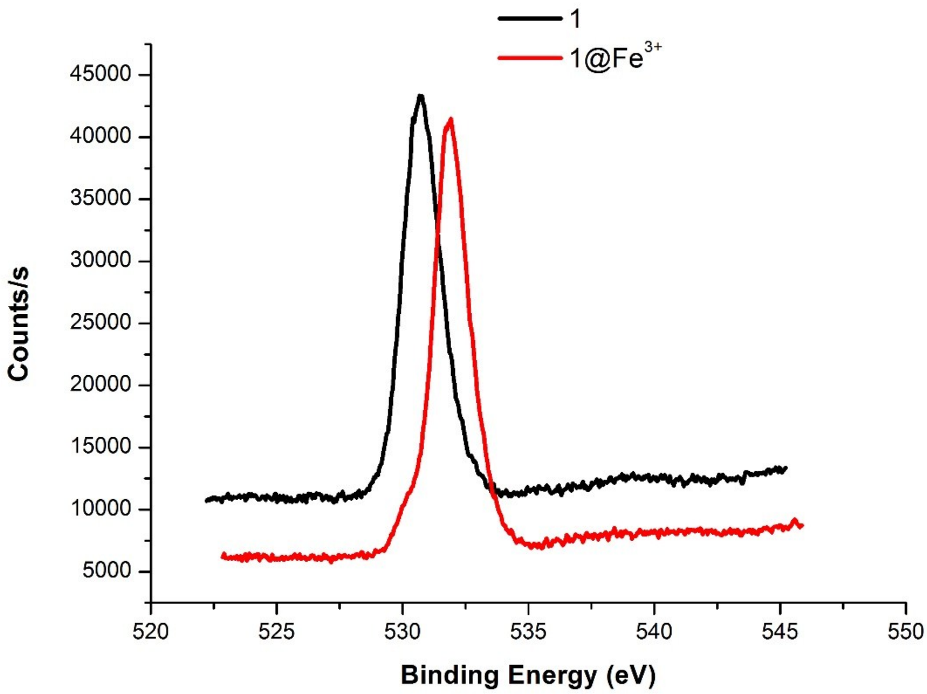

Fig. S30 The O1s XPS spectra of the **1** (black) and **1**@Fe^{3+} (red).

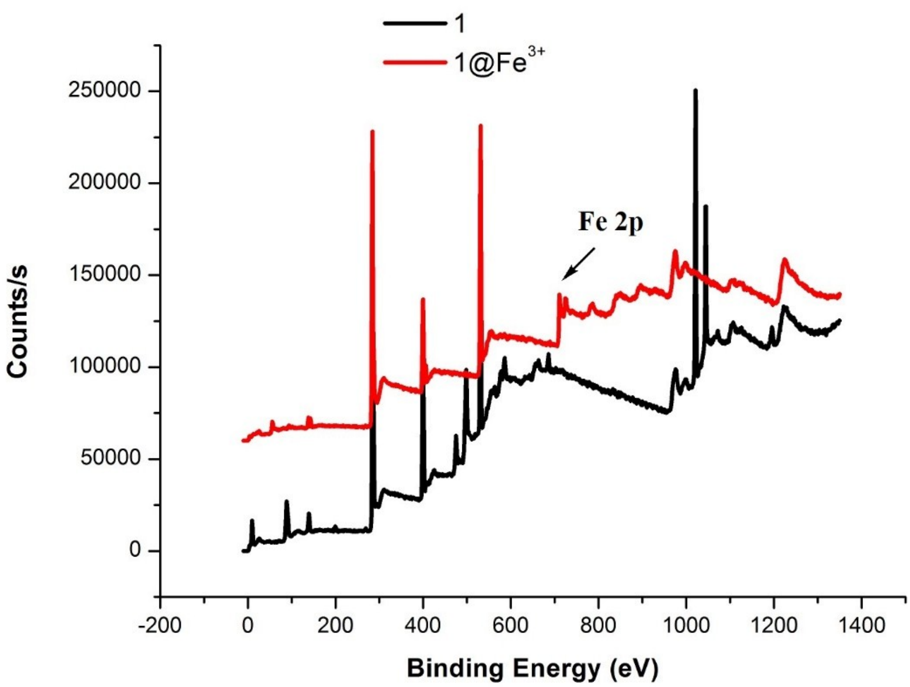

Fig. S31 The XPS spectra of the **1**@Fe^{3+} (red) and **1** (black).

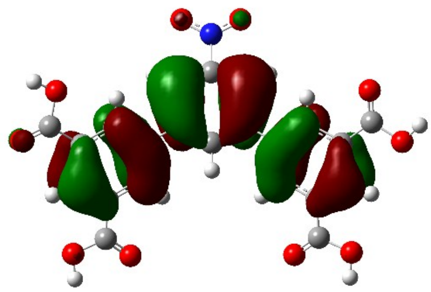

HOMO H_4ddn

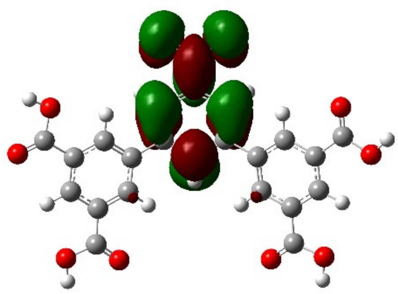

LUMO H_4ddn

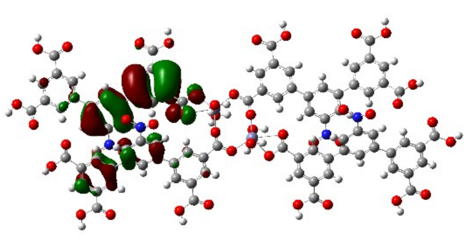

HOMO **1**

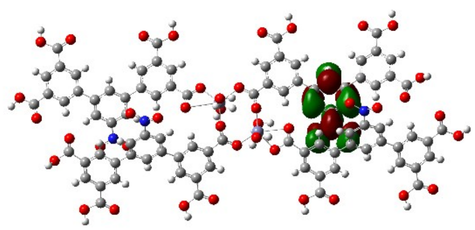

LUMO **1**

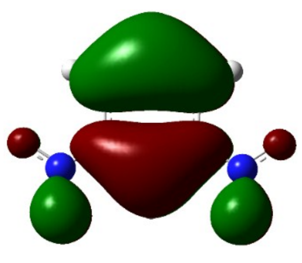

HOMO 1,3-DNB

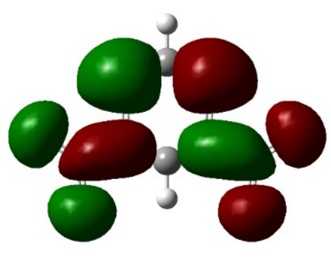

LUMO 1,3-DNB

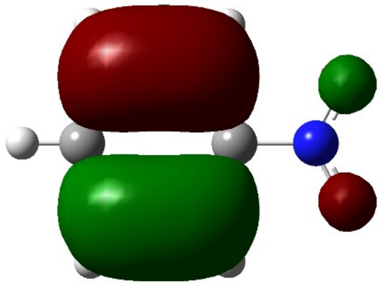

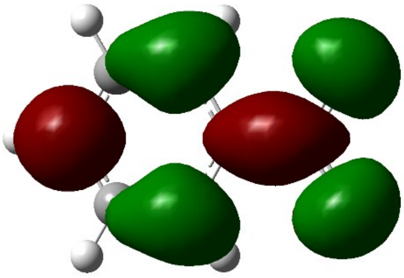

HOMO NB

LUMO NB

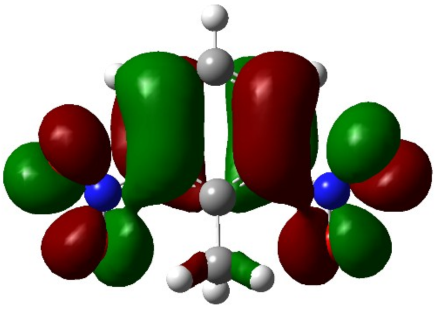

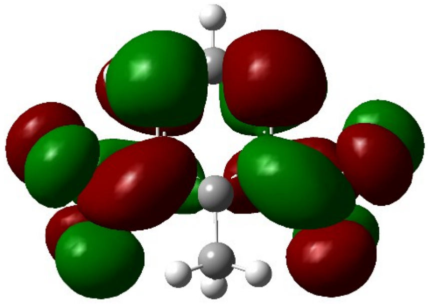

HOMO 2,6-DNT

LUMO 2,6-DNT

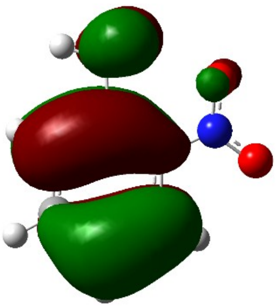

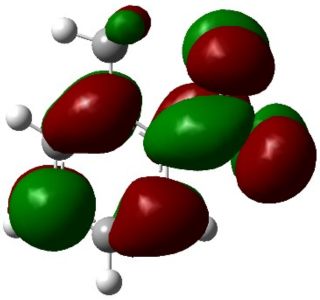

HOMO 2-NT

LUMO 2-NT

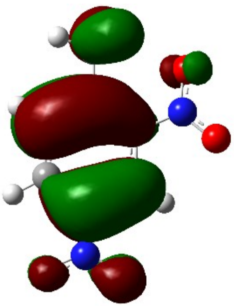

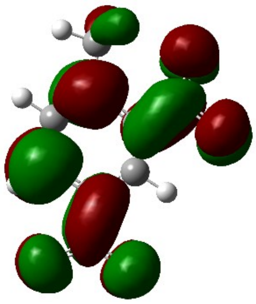

HOMO 2,4-DNT

LUMO 2,4-DNT

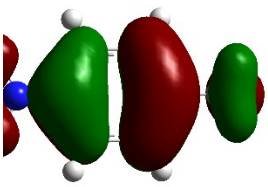

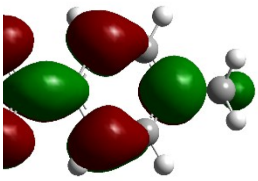

HOMO 4-NT

LUMO 4-NT

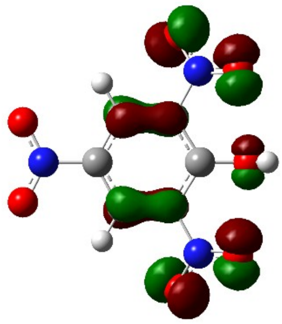

HOMO TNP

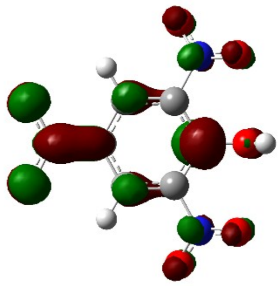

LUMO TNP

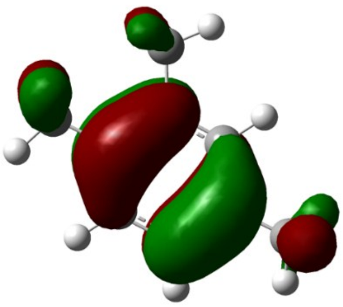

HOMO 1,2,4-TMB

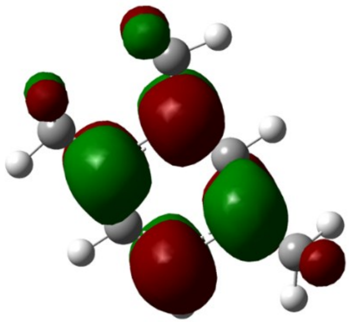

LUMO 1,2,4-TMB

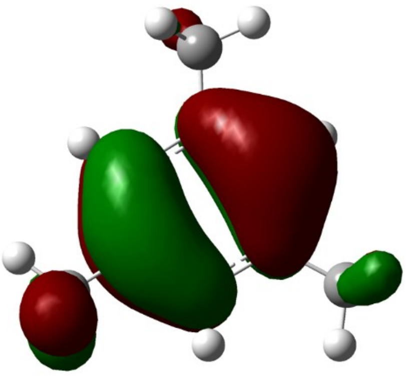

HOMO 1,3,5-TMB

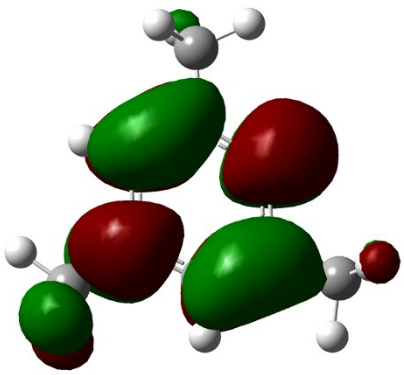

LUMO 1,3,5-TMB

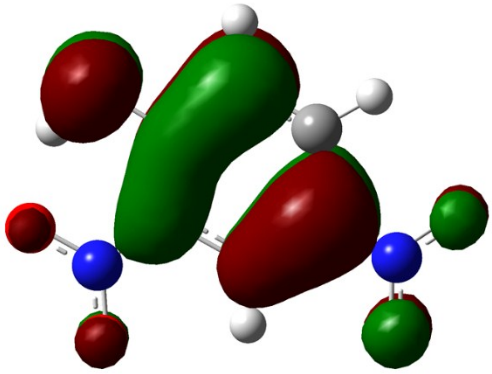

HOMO 2,4-DNP

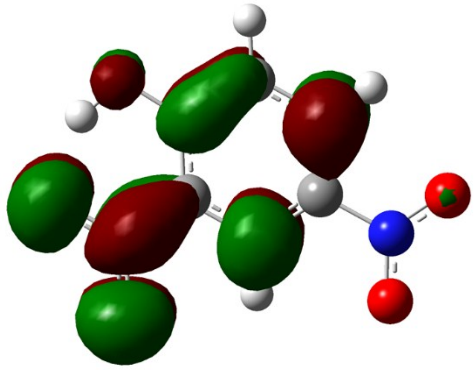

LUMO 2,4-DNP

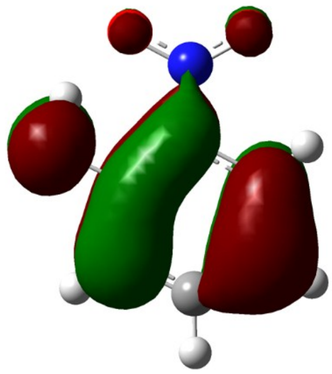

HOMO o-nitro phenol

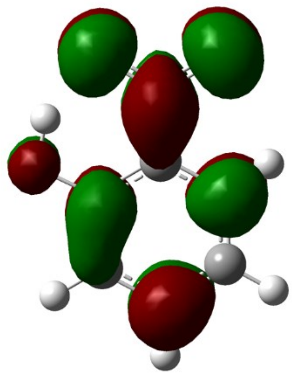

LUMO o-nitro phenol

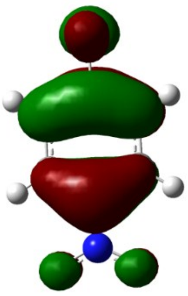

HOMO p-nitrophenol

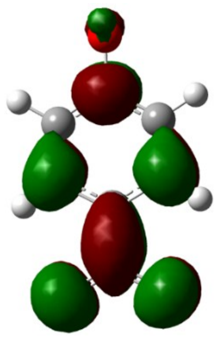

LUMO p-nitrophenol

Fig. S32 HOMO-LUMO plots for H_4ddn, **1** and aromatic analytes.

Table S1 Crystal data and structure refinement for 1

Empirical formula	$C_{44}H_{19}N_3O_{26}Zn_4$
Formula weight	1267.10
Temperature/K	150.00(10)
Crystal system	orthorhombic
Space group	$P2_12_12_1$
a/Å	17.4270(2)
b/Å	22.7852(8)
c/Å	25.2350(7)

α/°	90
β/°	90
γ/°	90
Volume/Å^3	10020.3(5)
Z	4
ρ_{calc}g/cm^3	0.840
μ/mm^{-1}	1.499
F(000)	2528.0
Index ranges	$-21 \leq h \leq 20$, $-14 \leq k \leq 28$, $-26 \leq l \leq 31$
Reflections collected	38476
Independent reflections	18163 R_{int} = 0.0438, R_{sigma} = 0.0641]
Data/restraints/parameters	18163/115/694
Goodness-of-fit on F^2	0.855
Final R indexes [I>=2σ (I)]	R_1 = 0.0455, wR_2 = 0.1078
Final R indexes [all data]	R_1 = 0.0736, wR_2 = 0.1208
Largest diff. peak/hole / e Å^{-3}	0.45/-0.38
Flack parameter	0.407(17)

Table S2 Bond Lengths and angles for 1

Zn01- Zn02^1	2.9459(6)	Zn01-	O16^2	2.002(3)
Zn01- O7^3	1.943(4)	Zn01-	O23	1.952(3)
Zn01- O3^4	2.101(4)	Zn01-	O20	2.041(5)
Zn02- O24	1.958(3)	Zn02-	O15^5	2.002(3)
Zn02- O4^3	2.064(4)	Zn02-	O19^2	2.003(4)
Zn02- O8^6	2.052(4)	Zn03-	O14	1.931(6)
Zn03- O1^5	2.030(5)	Zn03-	O10	2.020(4)
Zn03- O11	2.060(7)	Zn03-	O12	2.146(7)
Zn04- O21^7	1.925(4)	Zn04-	O9	1.747(9)

O16^1- Zn01- O20	160.93(13)
O24- Zn02- O44	103.16(14)
O24- Zn02- O86	95.00(14)
O14- Zn03- O1^5	141.05(17)
O11- Zn03- O12	173.5(2)
O21- Zn04- O13	86.9(3)

O9- Zn04- O217 128.5(3)

---

[1]1/2+X,1/2-Y,2-Z; [2]-1/2+X,1/2-Y,2-Z; [3]1-X,-1/2+Y,3/2-Z; [4]3/2-X,1-Y,1/2+Z; [5]1+X,+Y,+Z; [6]2-X,-1/2+Y,3/2-Z; [7]-1+X,+Y,+Z

Table S3 Comparison of the selected materials in detective sensitivity for Fe^{3+} ions

Material	Sensitivity	Reference
$Eu(acac)_3@Zn(C_{15}H_{12}NO_2)_2$	5×10^{-3} M	1
$Eu(C_{33}H_{24}O_{12})(H_2NMe)(H_2O)$	2×10^{-4} M	2
$Eu(C_{22}H_{14}O_2)_3$	10^{-4} M	3
$[Eu(BTPCA)(H_2O)]\cdot2DMF\cdot3H_2O$	10^{-5} M	4
MIL-53(Al)	0.9×10^{-6} M	5
$\{[LnCd_2(DTPA)_2(H_2O)_4]\cdot4H_2O$	1.5×10^{-5} M	6
carbon nanoparticles (CNPs)	0.32×10^{-6} M	7
Fluorescent Gold Nanoclusters	5.4×10^{-6} M	8
$[Cd_3(dpa)(DMF)_2(H_2O)_3]\cdot DMF$	1.75×10^{-4} M	9
$Zn_3L_3(DMF)_2$	10^{-5} M	10
$[[Eu_2(MFDA)_2(HCOO)_2(H_2O)_6]\cdot H_2O$	1.0×10^{-4} M	11
$[Tb_4(OH)_4(DSOA)_2(H_2O)_8]\cdot(H_2O)_8$	10^{-6} M	12
$[H_2N(Me)_2][Eu_3(OH)(bpt)_3(H_2O)_3](DMF)_2\cdot(H_2O)_4$	10^{-5} M	13
$[Eu_2(MFDA)_2(HCOO)_2(H_2O)_6]\cdot H_2O$	10^{-5} M	14
TbL	10^{-6} M	15
$[Eu(HL)(H_2O_2)]\cdot2H_2O$	3.0×10^{-4} M	16
1	2.3×10^{-5} M	*In this work*

References:

[1] G. G. Hou, Y. Liu, Q. K. Liu, J. P. Ma and Y. B. Dong, *Chem. Commun.*2011, ***47***, 10731-10733.

[2] S. Dang, E. Ma, Z.M. Sun and H. J. Zhang, *J. Mater. Chem.* 2012, ***22***, 16920-16926.

[3] M. Zheng, H. Q. Tan, Z. G. Xie, L. G. Zhang, X. B. Jing and Z. C. Sun, *ACS Appl. Mater. Interfaces,* 2013, ***5***, 1078-1083.

[4] Q. Tang, S. X. Liu, Y. W. Liu, J. Miao, S. J. Li, L. Zhang, Z. Shi and Z. P. Zheng, *Inorg. Chem.*2013, ***52***, 2799-2801.

[5] C. X. Yang, H. B. Ren and X. P. Yan, *Anal. Chem.*2013, ***85***, 7441-7446.

[6] Q. Liu, F. Wan, L. X. Qiu, Y. Q. Sun and Y. P. Chen, *RSC Adv*., 2014, ***4***, 27013-27021.

[7] K. G. Qu, J. S. Wang, J. S. Ren and X. G. Qu, *Chem. Eur. J.* 2013, ***19***, 7243-7249.

[8] J.-A. A. Ho, H.-C. Chang and W.-T. Su, *Anal. Chem*. 2012, ***84***, 3246-3253.

[9] J. C. Jin, L. Y. Pang, G. P. Yang, L. Hou and Y. Y. Wang, *Dalton Trans*., 2015,

44, 17222–17228.
[10] Z. C. Yu, F. Q. Wang, X. Y. Lin, C. M. Wang, Y. Y. Fu, X. J. Wang, Y. N. Zhao and G. D. Li, *J. Solid. State. Chem*., 2015, ***232***, 96-101.
[11] X. H. Zhou, L. Li, H. H. Li, T. Yang and W. Huang, *Dalton Trans*., 2013, **42**, 12403–12409.
[12] X. Y. Dong, R. Wang, J. Z. Wang, S. Q. Zang and T. C. W. Mak, *J. Mater. Chem*. A, 2015, ***3***, 641–647.
[13] S. Xing, Q. Bing, L. Song, G. Li, J. Liu, Z. Shi, S. Feng and R. Xu, *Chem. – Eur. J.*, 2016, **22**, 16230-16235.
[14] X. Zhou, L. Li, H. Li, A. Li, T. Yang and W. Huang, *Dalton Trans.,* 2013, **42**, 12403-12409.
[15] S. Dang, T. Wang, F. Yi, Q. Liu, W. Yang and Z. Sun, *Chem. – Asian J.*, 2015, **10**, 1703-1709.
[16] Y. Liang, G. Yang, B. Liu, Y. Yan, Z. Xi and Y. Wang, *Dalton Trans.,* 2015, **44**, 13325-13330.